THE JOURNAL OF BIOLOGICAL CHEMISTRY VOL. 289, NO. 41, pp. 28149–28159, October 10, 2014

Metal Bridges Illuminate Transmembrane Domain Movements during Gating of the Cystic Fibrosis Transmembrane Conductance Regulator Chloride Channel*

Received for publication, June 30, 2014, and in revised form, July 25, 2014 Published, JBC Papers in Press, August 20, 2014, DOI 10.1074/jbc.M114.593103

Yassine El Hiani and Paul Linsdell[1]

From the Department of Physiology and Biophysics, Dalhousie University, Halifax, Nova Scotia B3H 4R2, Canada

Background: Opening and closing of the CFTR channel involve conformational changes in the channel pore.
Results: Different metal bridges stabilize the channel in the open or closed configuration.
Conclusion: Opening and closing result from relative lateral movement of different transmembrane segments.
Significance: This work defines the three-dimensional conformational changes underlying channel opening and closing.

Opening and closing of the cystic fibrosis transmembrane conductance regulator are controlled by ATP binding and hydrolysis by the cytoplasmic nucleotide-binding domains. Different conformational changes in the channel pore have been described during channel opening and closing; however, the relative importance of these changes to the process of gating the pore is not known. We have used patch clamp recording to identify high affinity Cd^{2+} bridges formed between pairs of pore-lining cysteine residues introduced into different transmembrane α-helices (TMs). Seven Cd^{2+} bridges were identified forming between cysteines in TMs 6 and 12. Interestingly, each of these Cd^{2+} bridges apparently formed only in closed channels, and their formation stabilized the closed state. In contrast, a single Cd^{2+} bridge identified between cysteines in TMs 1 and 12 stabilized the channel open state. Analysis of the pattern of Cd^{2+} bridge formation in different channel states suggests that lateral separation and convergence of different TMs, rather than relative rotation or translation of different TMs, is the key conformational change that causes the channel pore to open and close.

Cystic fibrosis is caused by loss-of-function mutations in the cystic fibrosis transmembrane conductance regulator (CFTR),[2] a phosphorylation-regulated, nucleotide-gated Cl^- channel found in the apical membrane of many epithelial cell types (1). CFTR is a member of the ATP-binding cassette (ABC) family of membrane transport proteins, with an archetypal architecture of two membrane-spanning domains (MSDs), each made up of six transmembrane α-helices (TMs) and two cytoplasmic nucleotide-binding domains (NBDs) (see Fig. 1). CFTR also contains a unique cytoplasmic regulatory domain. Opening and closing of phosphorylated CFTR channels are controlled by ATP binding and hydrolysis by a dimer of the two NBDs; this is presumed to result in the opening and closing of a gate within the MSDs that allows or prevents the transmembrane movement of Cl^- and other small anions (2, 3). However, the overall structure of the channel pore formed by the MSDs, the location of the gate, and the structural rearrangements that occur within the pore region that control gate opening and closing are not known.

The channel pore is lined by a subset of the TMs, with TMs 1, 6, and 12 playing particularly important functional roles (2, 3) (see Fig. 1). At the functional level, the pore is divided into a central narrow region flanked by wider inner and outer vestibules (3). The contributions of different TMs, and specific amino acid side chains coming from different TMs, to each of these functionally distinct, two-dimensional regions of the pore has been reviewed recently (3); however, the three-dimensional structure of the pore is less well defined experimentally. Three-dimensional atomic homology models of CFTR have been generated based on related, non-ion channel ABC proteins (4–6); however, the structures of the pore suggested by these models show some important discrepancies from functional models based on direct experimental evidence (3).

The three-dimensional structure of the pore is not static but presumably changes as the channel opens and closes. Indeed, different conformational changes of the pore during channel gating have been proposed (2, 3). These include local constrictions/dilations of the pore (7–10), as well as rotational (11, 12) and translational (7) movements of individual TMs. However, although experimental evidence for these different kinds of movement has been put forward, the relative mechanistic importance of these movements for the process of channel opening and closing is not known. Evidence for conformational changes in individual TMs within the inner vestibule of the pore during channel gating is mainly two-dimensional in nature, coming from state-dependent differences in the accessibility of cytoplasmically applied cysteine reactive methanethiosulfonate reagents to cysteine side chains introduced into TMs 1 (8, 9, 13, 14), 6 (8, 9, 11, 15), 11 (10), and 12 (12, 16). However, how the relative positions of these TM changes in three-dimensional space during channel gating have not previously been investigated.

* This work was supported by the Canadian Institutes of Health Research.
[1] To whom correspondence should be addressed: Department of Physiology and Biophysics, Dalhousie University, P. O. Box 15000, Halifax, Nova Scotia B3H 4R2, Canada. Tel.: 902-494-2265; Fax: 902-494-1685; E-mail: paul.linsdell@dal.ca.
[2] The abbreviations used are: CFTR, cystic fibrosis transmembrane conductance regulator; ABC, ATP-binding cassette; MSD, membrane-spanning domain; NBD, nucleotide-binding domain; TM, transmembrane α-helix.

Direct information concerning the three-dimensional structure of the pore has come from disulfide cross-linking experiments (7, 13, 17), as well as from experiments in which anionic channel blocker binding was altered by introduction of positively charged amino acid side chains (17, 18). Previously, we have used the oxidizing agent copper(II)-*o*-phenanthroline to show that disulfide bonds can be formed between cysteine side chains introduced into different TMs, and we used this information to infer the relative proximity of residues in these different TMs lining the inner vestibule of the pore (13, 17). However, because these disulfide bonds are essentially irreversible under non-reducing conditions, this approach has several disadvantages, such as the potential for disulfide bonds to form during rare or unnatural channel conformations when normally distant cysteine side chains transiently approach close together. Furthermore, the irreversible nature of disulfide bonds makes it difficult to investigate state-dependent changes in the proximity of pairs of cysteine side chains. An alternative approach is to use weaker Cd^{2+} bridges that are more likely to catch the channel in native conformations (19–22). An additional advantage is that these weaker, reversible interactions can break and reform, allowing channel gating to proceed relatively normally (22) and so potentially providing information on the relative propensity of Cd^{2+} bridges to form in different gating states. In the present study, we have investigated the potential of Cd^{2+} to form metal bridges between nearby pore-lining cysteine side chains introduced into TMs 1, 6, and 12 lining a localized region of the inner vestibule of the channel pore close to an anionic blocker-binding site (17, 18). In particular, we have taken advantage of the dynamic nature of Cd^{2+} bridges to associate the formation of these bridges with different channel conformational states. Our results show that Cd^{2+} bridges form selectively between a limited number of cysteine pairs in TMs 6 and 12, suggesting a relative alignment of these two TMs. Interestingly, each of these bridges appears to form only in closed channels, and they stabilize the channel in the closed state. In contrast, a single identified Cd^{2+} bridge between TMs 1 and 12 stabilized the channel in the open state. These results support a model in which relative lateral movement of different TMs toward and away from each other in the inner vestibule, rather than helical rotation or translation of individual TMs, is required for the channel to open and close.

EXPERIMENTAL PROCEDURES

Experiments were carried out in baby hamster kidney cells transiently transfected with CFTR. In this study, we have used a human CFTR variant in which all cysteines had been removed by mutagenesis (as described in Ref. 23) and that includes a mutation in NBD1 (V510A) to increase protein expression in the cell membrane (24). This Cys-less variant, which we have used in previous studies of pore conformational change (7–9), has functional properties that are very similar to those of wild-type CFTR (25). Additional mutations were introduced into the Cys-less background using the QuikChange site-directed mutagenesis system (Agilent Technologies, Santa Clara, CA) and verified by DNA sequencing. In some cases, cysteine mutants were combined with the NBD2 mutation E1371Q, which we (7–9) and others (12, 26) have used to abolish ATP-dependent channel gating and lock CFTR channels in the open state. In our expression system, the open probability of channels bearing the E1371Q mutation is >95% (7).

To investigate potential Cd^{2+} bridges formed between pore-lining cysteine side chains exposed in the inner vestibule of the CFTR pore, we combined individual cysteines that we previously found to be accessible to cytoplasmically applied methanethiosulfonate reagents in three important pore-lining TMs: TM1 (K95C, Q98C) (13), TM6 (I344C, V345C, M348C, A349C) (15), and TM12 (M1140C, S1141C, T1142C, Q1144C, W1145C, V1147C, N1148C) (16), to generate a total of 50 double cysteine mutants (8 TM1:TM6; 14 TM1:TM12; 28 TM6:TM12).

Macroscopic CFTR currents were recorded using patch clamp recordings from inside-out membrane patches, as described in detail recently (17). Following patch excision and recording of background currents, CFTR channels were activated by exposure to protein kinase A catalytic subunit (PKA; 20 nM) plus MgATP (1 mM) in the intracellular solution. In some cases (see Fig. 4), patches were subsequently treated with 2 mM sodium pyrophosphate (PP_i) to stabilize the channel open state (27, 28), as described previously in studies of state-dependent modification of Cys-less CFTR (8, 15). Both intracellular (bath) and extracellular (pipette) solutions contained (in mM): 150 NaCl, 2 $MgCl_2$, 10 *N*-tris[hydroxymethyl]methyl-2-aminoethanesulfonate, pH 7.4. Current traces were filtered at 100 Hz using an eight-pole Bessel filter, digitized at 250 Hz, and analyzed using pCLAMP software (Molecular Devices, Sunnyvale, CA). CFTR current amplitudes were monitored during brief voltage deflections (to ±50 mV) from a holding potential of 0 mV applied every 6 s (10). In some cases, the identity of CFTR currents in inside-out patches was confirmed by their sensitivity to the specific inhibitor $CFTR_{inh}$-172 (5 μM). Different concentrations of $CdCl_2$ were applied directly to the cytoplasmic face of inside-out patches from stock solutions made up in normal intracellular solution. In those cases where exposure to Cd^{2+} caused inhibition of current amplitude, concentration-inhibition relationships were fitted by the equation.

$$\text{Fractional unblocked current} = 1/(1 + ([Cd^{2+}]/K_i)) \quad \text{(Eq. 1)}$$

Experiments were carried out at room temperature (21–24 °C). The values are presented as the means ± S.E. Tests of significance were carried out using an unpaired *t* test, with $p < 0.05$ being considered statistically significant. All chemicals were from Sigma-Aldrich, except for PKA (Promega, Madison, WI).

RESULTS

Metal Bridge Formation between TMs 6 and 12—Pore-lining TMs 6 and 12 make important functional contributions to the inner vestibule of the pore (2, 3) and occupy symmetrical positions within the MSDs (Fig. 1). To investigate the potential for Cd^{2+} bridge formation between pore-forming side chains coming from TMs 6 and 12, we introduced cysteines at each of four sites in TM6 (Ile-344, Val-345, Met-348, Ala-349) and seven sites in TM12 (Met-1140, Ser-1141, Thr-1142, Gln-1144, Trp-1145, Val-1147, Asn-1148) that we have previously found to be accessible to cysteine-reactive methanethiosulfonate reagents

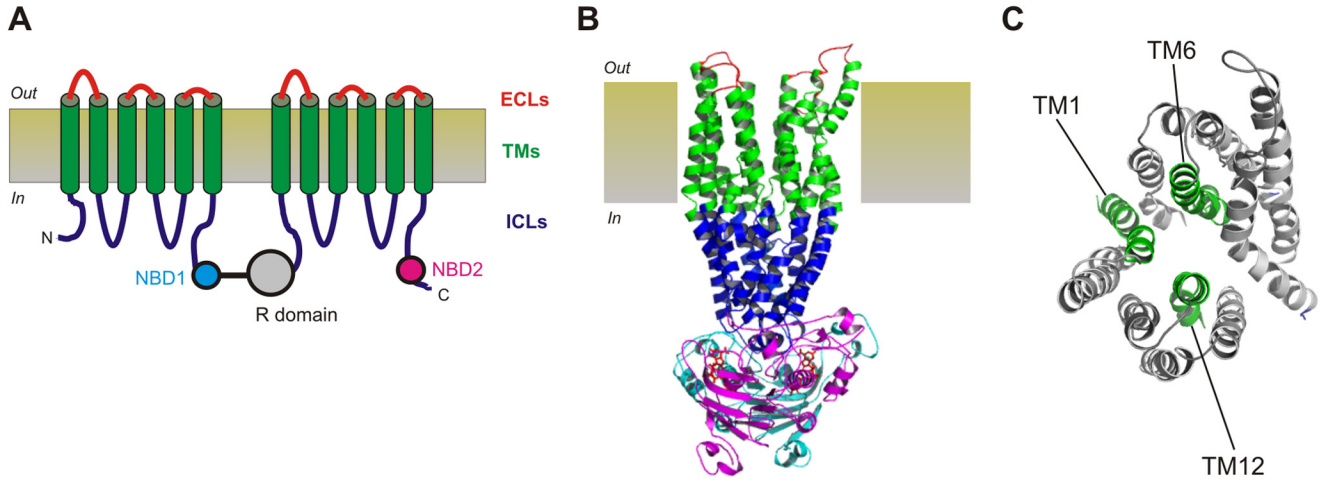

FIGURE 1. **Putative structure of the CFTR channel pore region.** *A*, graphic model of CFTR structure, consisting of 12 TMs (*green*), two NBDs (NBD1, *cyan*; NBD2, *magenta*), the cytoplasmic R domain (*gray*), six extracellular loops (*ECLs*, *red*), and four intracellular loops (*ICLs*, *blue*). *B*, so-called "channel-like" atomic homology model of CFTR structure (6), based on the bacterial ABC protein Sav1866 and showing the approximate extent of the extracellular loops, TMs, intracellular loops, and NBDs using the same color scheme as in *A*. The R domain is absent from this model. *C*, location of putative pore-lining TMs 1, 6, and 12 within the MSDs of this same homology model, viewed from the extracellular side of the membrane. CFTR model structures were visualized with PyMOL (33) using coordinates provided by Ref. 6.

applied to the cytoplasmic side of the membrane (15, 16). Combination of each single cysteine mutant from each TM then gave a total of 28 double-cysteine mutants containing one cysteine in TM6 and one cysteine in TM12 within the putative inner vestibule of the pore.

Cys-less CFTR itself was weakly inhibited by the addition of millimolar concentrations of Cd^{2+} to the cytoplasmic side of the membrane (Fig. 2, *A* and *B*), presumably acting in a cysteine-independent manner. All 11 single cysteine mutants tested were more strongly inhibited by Cd^{2+} (Fig. 2, *A* and *B*), with estimated K_i values in the range of 70–250 μM (Fig. 3). This suggests that Cd^{2+} is able to bind to each of these introduced cysteine side chains (29), which is consistent with the proposed pore-lining location of the cysteine residues introduced. The effects of Cd^{2+} appeared independent of voltage (Fig. 2, *A* and *B*).

Of the 28 double-cysteine mutants tested, most (twenty-one) did not result in an increase in sensitivity to Cd^{2+} as compared with the corresponding single-cysteine mutants (Fig. 4). In contrast, the remaining seven double cysteine mutants, namely I344C/S1141C (Fig. 2, *C* and *D*), V345C/S1141C, M348C/S1141C (Fig. 2, *C* and *E*), M348C/V1144C, M348C/W1145C, M348C/V1147C, and M348C/N1148C, all showed increased sensitivity to Cd^{2+}, leading to a significant decrease in K_i as compared with either of the single cysteine mutants from which they were derived (estimated K_i values < 50 μM; Fig. 3). In theory, this apparent increase in Cd^{2+} potency could reflect additive effects of two Cd^{2+} ions bound simultaneously to different cysteine side chains. However, if the inner vestibule of the pore were able to accommodate two Cd^{2+} ions simultaneously, we would expect most double cysteine mutants to show strong Cd^{2+} binding, especially where the two cysteine side chains are expected to be relatively far apart (see "Discussion"). Instead, we propose that the relatively small number of double cysteine mutant channels that show strengthened Cd^{2+} binding results from specific coordination of a single Cd^{2+} ion interacting simultaneously with both cysteine side chains. This proposal is consistent with recent studies showing that cysteine side chains introduced into ion channel pores bind a single Cd^{2+} ion and that nearby cysteine side chains then increase the strength of binding of this single Cd^{2+} ion (29). In effect, those combinations of cysteine pairs that led specifically to a strengthened binding of Cd^{2+} within the pore (but no other combination of cysteines tested) are proposed to support the formation of Cd^{2+} bridges between TMs 6 and 12 that impair channel function. In particular, M348C/S1141C was associated with a dramatic increase in sensitivity to Cd^{2+} (Fig. 2, *C* and *E*, and Fig. 3) with an estimated K_i of 0.14 ± 0.02 μM ($n = 5$).

The finding that Cd^{2+} bridges between TMs 6 and 12 inhibited channel function suggested to us that these bridges may stabilize the channel closed state. To test this idea, we applied Cd^{2+} following channel treatment with 2 mM PP_i to stabilize the channel open state (see "Experimental Procedures"). In each case, PP_i treatment resulted in a weakening of Cd^{2+} inhibition (Fig. 4*A*) and a significant increase in K_i (Fig. 4*B*) of between 2.3-fold (in I344C/S1141C) and 97-fold (in M348C/S1141C). This weakened interaction is consistent with Cd^{2+} normally interacting with the closed state of these mutant channels to impair channel opening. To confirm this apparent state dependence of Cd^{2+} bridge formation, we combined selected single and double cysteine mutants with the E1371Q mutation in NBD2 that results in constitutively open channels in our expression system (see "Experimental Procedures"). As shown in Fig. 5, all E1371Q-containing channels tested were only weakly sensitive to inhibition by Cd^{2+}, resulting in a significant increase in K_i both in single cysteine (I344C, M348C, S1141C) and in double cysteine (I344C/S1141C, Fig. 5, *A*–*C*; M348C/S1141C, Fig. 5, *A*, *D*, and *E*) mutant channels. However, the effect of the E1371Q mutation was greater in the double cysteine mutants; this gating mutation increased K_i 30-fold in I344C/S1141C (Fig. 5*C*) and 2500-fold in M348C/S1141C (Fig. 5*E*). In fact, in striking contrast to normally gating CFTR channels in which these double cysteine mutants showed greatly increased sensitivity to Cd^{2+} as compared with the correspond-

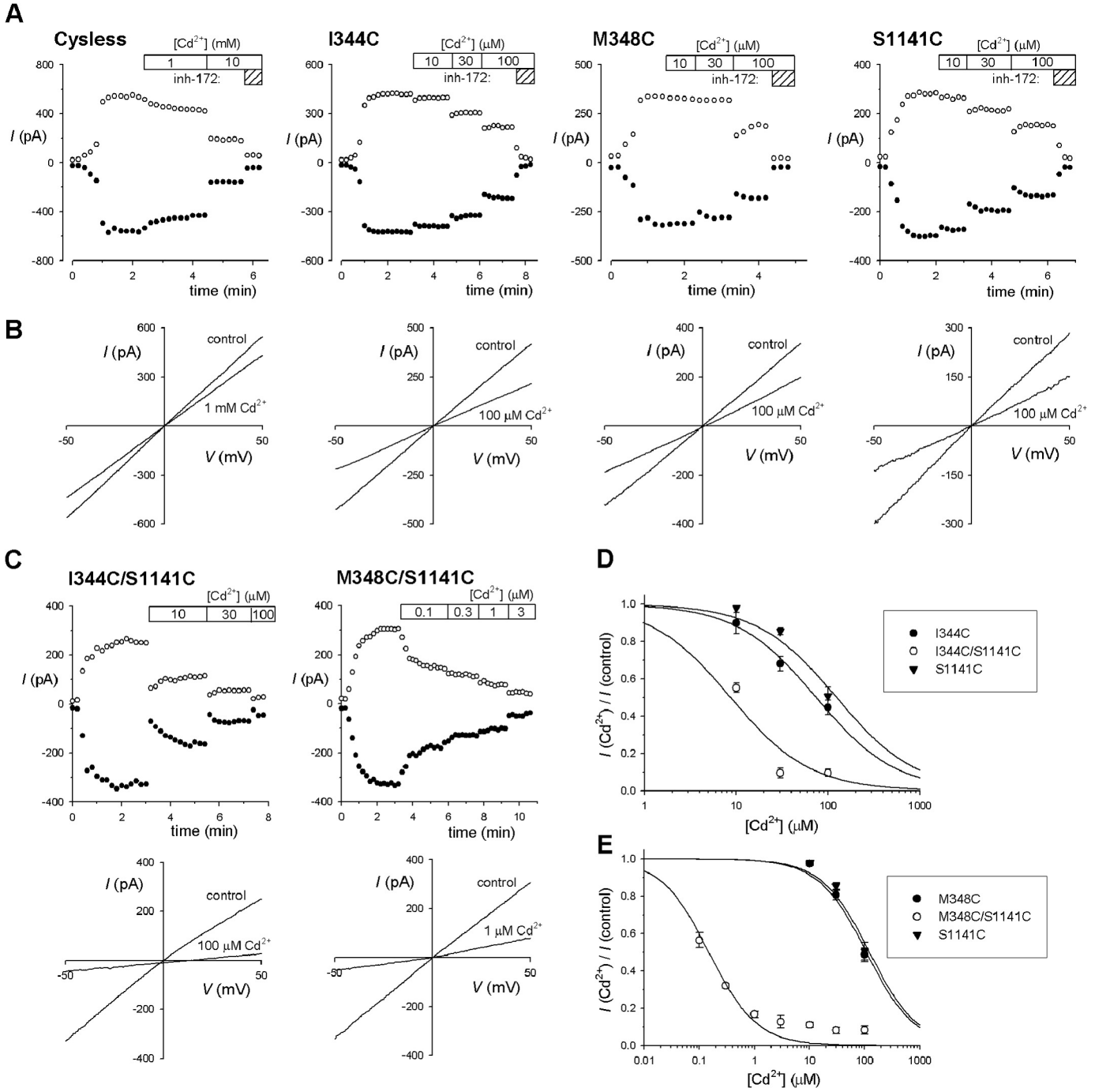

FIGURE 2. **Effects of Cd^{2+} on single and double cysteine mutant channels in TMs 6 and 12.** *A*, sample time courses of current activation (by PKA application in the presence of ATP, at time 0) and inhibition by Cd^{2+} (at the concentrations indicated at the *top* of each panel) for the named CFTR variants. Currents were monitored using depolarizing voltage ramps (*B*) and are plotted at −50 mV (●) and +50 mV (○). The identity of CFTR currents was confirmed by sensitivity to $CFTR_{inh}$-172 (5 μM; indicated by *hatched bars* marked *inh-172*). *B*, sample macroscopic *I-V* curves for these same four membrane patches, recorded before the addition of Cd^{2+} (*control*) and after the addition of the noted concentration of Cd^{2+}. *C*, sample time courses (*upper panels*) and *I-V* curves (*lower panels*) recorded from similar experiments for the double cysteine mutants I344C/S1141C (*left*) and M348C/S1141C (*right*). *D* and *E*, concentration-dependent inhibition of the single (*filled symbols*) and double (*open symbols*) cysteine mutants channels indicated, indicating the increase in Cd^{2+} apparent affinity when individual cysteine mutants in TMs 6 and 12 are combined. Data have been fitted as described under "Experimental Procedures." Mean of data from 3–9 patches. *Error bars* indicate the means ± S.E.

ing single cysteine mutants (Figs. 3 and Fig. 5, *C* and *E*), in E1371Q mutant channels, the K_i for the double cysteine mutants was not significantly different from the single cysteine mutants (Fig. 5, *B–E*). The finding that these cysteine pairs fail to increase Cd^{2+} sensitivity in constitutively open channels (relative to single cysteines) suggests that Cd^{2+} bridge formation effectively does not occur in the open state and supports the idea that the inhibitory effect of Cd^{2+} bridge formation between TMs 6 and 12 results from a specific interaction with, and resulting stabilization of, the channel closed state.

Metal Bridge Formation between TMs 1 and 6 and 12—In addition to TMs 6 and 12, TM1 also plays an important func-

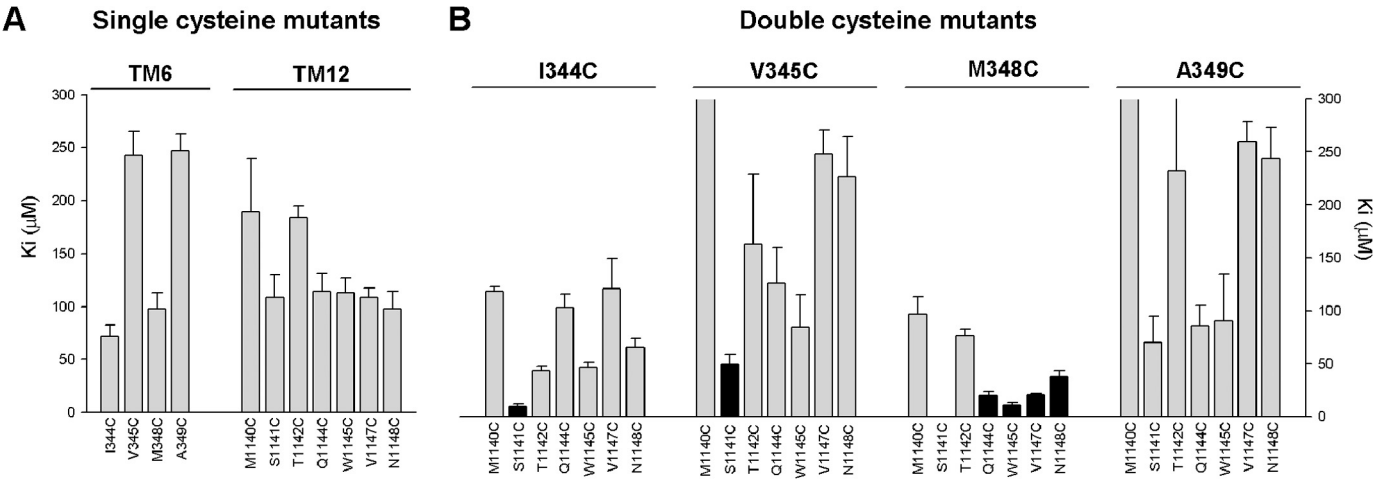

FIGURE 3. **Mean inhibitory effect of Cd^{2+} on single and double cysteine mutant channels in TMs 6 and 12.** Mean K_i values were calculated from fits to data from individual patches as those shown in Fig. 2, *D* and *E*. *A*, single cysteine mutants in TM6 (*left*) and TM12 (*right*) as indicated. *B*, double cysteine mutants that combine one cysteine substituted in TM6 (listed above the panel) with one in TM12 (listed below the panel). Those double mutants that showed a significantly different K_i from that of either of the corresponding single cysteine mutants ($p < 0.05$) are *filled black*, whereas those that with no significant difference are *filled gray*. Note that the K_i for M348C/S1141C (0.14 ± 0.02 μM, $n = 5$) is too small to be visible on this scale, but was significantly different from either M348C or S1141C alone ($p < 0.0005$; see also Fig. 2*E*). Also note that the estimated K_i values for some double mutants were ≥300 μM (V345C/M1140C, 316 ± 38 μM, $n = 3$; A349C/M1140C, 345 ± 58 μM, $n = 3$; A349C/T1142C, 231 ± 68 μM, $n = 3$). *Error bars* indicate the means ± S.E. from 3–7 patches.

tional role lining the inner vestibule (3, 13, 14). However, in our hands, fewer side chains from TM1 line the inner vestibule (13), and when investigating potential Cd^{2+} bridge formation involving this TM, we were limited to cysteines substituted at two positions (Lys-95 and Gln-98). Furthermore, in contrast to TM6:TM12 double cysteine mutants, in several cases, double mutants involving these sites in TM1 failed to express significant currents in inside-out membrane patches. As a result, we were only able to study 9 mutants combining cysteines in TMs 1 and 6, and 10 mutants combining cysteines in TMs 1 and 12.

In striking contrast to cysteine substitution in TMs 6 and 12, we found that K95C channel currents were weakly, but significantly, increased in amplitude by Cd^{2+} at concentrations of 30–100 μM (Fig. 6). Because K95C is the only single mutant we have studied that involves replacement of a positively charged amino acid side chain by cysteine, and because removal of this positive charge by mutagenesis is known to reduce single channel conductance by ~85% (17, 18, 30), we considered whether this apparent stimulatory effect of Cd^{2+} could result from a bound Cd^{2+} ion acting as a surrogate fixed positive charge in the pore and thereby increasing Cl^- conductance. If this were the case, Cd^{2+} should have a consistent stimulatory effect irrespective of channel gating. However, we found that constitutively open K95C/E1371Q channels were insensitive to Cd^{2+} at concentrations up to 100 μM (Fig. 6*B*), as were K95C channels following treatment with 2 mM PP_i (data not shown), inconsistent with an effect of Cd^{2+} on Cl^- conductance. Instead, these results suggest that Cd^{2+} binding to K95C results in a small but significant stabilization of the channel open state, an effect that is not observed in E1371Q channels that are already open almost 100% of the time (7). In contrast to these results with K95C, but in common with TMs 6 and 12 single cysteine mutants, Q98C channels were inhibited by Cd^{2+} (Fig. 7).

Most (18 out of 19) double cysteine mutants including K95C or Q98C were weakly inhibited by Cd^{2+}, consistent with Cd^{2+} effects on single cysteine mutants in TMs 6 or 12 (or indeed in Q98C) (Fig. 7). Thus, evidence for Cd^{2+} bridge formation involving TM1 is scant. However, one mutant, K95C/S1141C, was apparently stimulated by Cd^{2+} (Fig. 6*A*), and this stimulation was of a greater magnitude than that seen in the K95C single cysteine mutant (Figs. 6*C* and 7). This suggests that a Cd^{2+} bridge may form between K95C in TM1 and S1141C in TM12. As with K95C itself, the stimulatory effects of Cd^{2+} on K95C/S1141C were abolished by the E1371Q mutation (Fig. 6*C*) or by treatment with PP_i (data not shown), suggesting that the observed effects of Cd^{2+} are due to an increase in channel open probability and a stabilization of the channel open state. Thus, although Cd^{2+} bridges between TMs 6 and 12 consistently stabilize the closed state, this single Cd^{2+} bridge between TMs 1 and 12 appears to stabilize the channel in the open state.

DISCUSSION

The inner vestibule of the CFTR channel pore is lined by TMs 1, 6, and 12 (3); however, their relative arrangement in three-dimensional space is not known. Consistent with their known pore-forming roles, cysteine residues introduced into each of 13 putative pore-lining positions in these three TMs resulted in macroscopic current sensitivity to submillimolar concentrations of cytoplasmically applied Cd^{2+} ions (Figs. 3*A* and 7) that was not observed in Cys-less background channels (Fig. 2). Similar Cd^{2+} sensitivity has previously been described for cysteine mutants in other parts of the pore (7, 26) and presumably reflects Cd^{2+} ion binding to these 13 different pore-exposed cysteine side chains (29). Channels bearing two cysteine residues, one in each of two different TMs, were also sensitive to cytoplasmic Cd^{2+} (Figs. 3*B* and 7). In most cases, combining two cysteines in different TMs did not lead to a significant change in apparent Cd^{2+} binding (Figs. 3*B* and 7), suggesting that the two cysteine side chains in question were unable to act together to coordinate Cd^{2+} binding, and also that simultaneous binding of two Cd^{2+} ions to both cysteines in this localized region of the pore is unlikely. However, in a limited

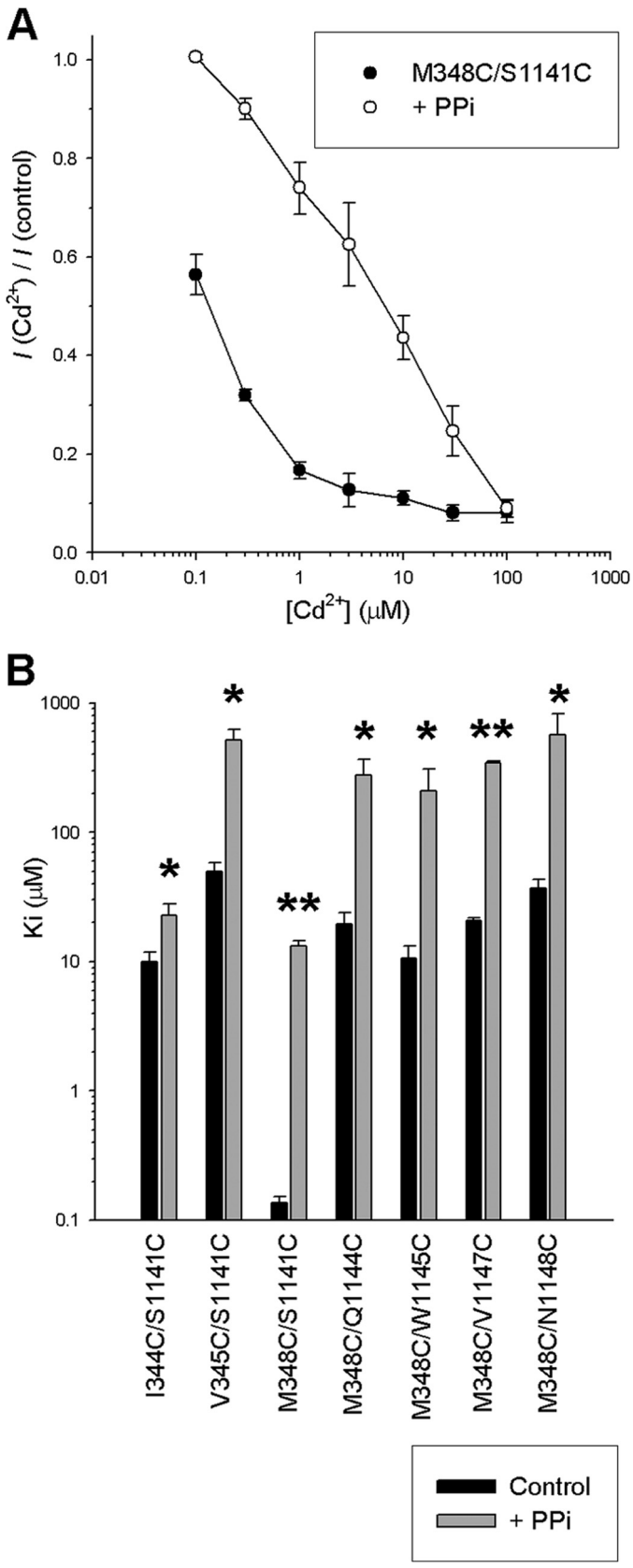

FIGURE 4. **Effect of increasing channel open probability with PP_i on Cd^{2+} sensitivity of TM6:TM12 double cysteine mutant channels.** *A*, mean fractional current remaining following the addition of different concentrations of Cd^{2+} in M348C/S1141C channels in the presence of PKA and ATP (●) or following activation by PKA and ATP followed by treatment with 2 mM PP_i to maximize channel open probability (○). *B*, mean K_i values estimated for the double cysteine mutant channels listed, either in the presence of PKA and ATP (*black bars*) or following treatment with PP_i (*gray bars*). *Asterisks* indicate a significant difference in the presence of PP_i (*, $p < 0.05$; **, $p < 0.00005$). *Error bars* indicate the means ± S.E. from 3–7 patches.

number of cases, double cysteine mutants exhibited tighter Cd^{2+} binding than either of the single cysteine mutants from which they were derived (Fig. 3). In highly localized regions of ion channel pores, this is generally considered consistent with the formation of a metal bridge between the two cysteine side chains (29). Indeed, the ability of a restricted subset of cysteine pairs specifically to coordinate binding of a single Cd^{2+} ion in the inner vestibule is consistent with the proposed alignment of TMs 1, 6, and 12 around this region of the pore (Fig. 8*A*). In contrast, binding of a second Cd^{2+} ion would be expected to be favored when two cysteine side chains were further apart, when simultaneously bound Cd^{2+} ions would be expected to experience less steric and electrostatic interference.

Of eight putative Cd^{2+} bridges identified (out of a total of 50 double cysteine mutants tested), all involved a cysteine substituted either for Met-348 (TM6) or for Ser-1141 (TM12) (Fig. 8*A*). Furthermore, when cysteine was present at both of these positions, an unusually high affinity Cd^{2+} bridge was formed (Figs. 2–5). These results suggest that cysteine side chains substituted for Met-348 or Ser-1141 are particularly well positioned to form inter-TM Cd^{2+} bridges.

Consideration of the different Cd^{2+} bridges that can form between different TMs may provide some information on the relative alignment and orientation of these TMs. Thus, M348C is able to form Cd^{2+} bridges with cysteines at multiple positions in TM12 (S1141C, Q1144C, W1145C, V1147C, N1148C) (Fig. 8*B*), and S1141C is able to form Cd^{2+} bridges with cysteines both in TM1 (K95C) and in TM6 (I344C, V345C, M348C) (Fig. 8*C*). The variety of bridges that can be formed from these two positions suggests that some degree of conformational flexibility must exist within these TMs. For example, M348C is able to form Cd^{2+} bridges with TM12 sites on a broad face of the TM12 helical face (Fig. 8*B*, *top panel*), suggesting some degree of relative rotational flexibility or movement, and also across a distance spanning two helical turns (from Ser-1141 to Asn-1148) (Fig. 8*B*, *bottom panel*), suggesting also some translational flexibility or movement. Similarly, S1141C is able to form Cd^{2+} bridges with different sites in TM6 (Fig. 8*C*). Thus, our results suggest that different TMs surrounding the inner vestibule do not occupy rigid positions relative to one another. Cadmium bridges between cysteine side chains are thought to require sulfur distances <6.5 Å (31).

Seven different Cd^{2+} bridges were identified as forming between cysteine side chains in TMs 6 and 12 (Figs. 3*B* and 8*A*). Interestingly, all of these Cd^{2+} bridges appear to form preferentially in the closed state and to stabilize the channel in this state. Thus, if channels are stabilized in the open state, either using PP_i to manipulate NBD-driven gating (Fig. 4) or using E1371Q channels that cannot hydrolyze ATP (Fig. 5), the inhibitory effects of Cd^{2+} are greatly reduced, suggesting that Cd^{2+} binds more strongly to the closed state than to the open state. Most striking in this respect was the M348C/S1141C mutant

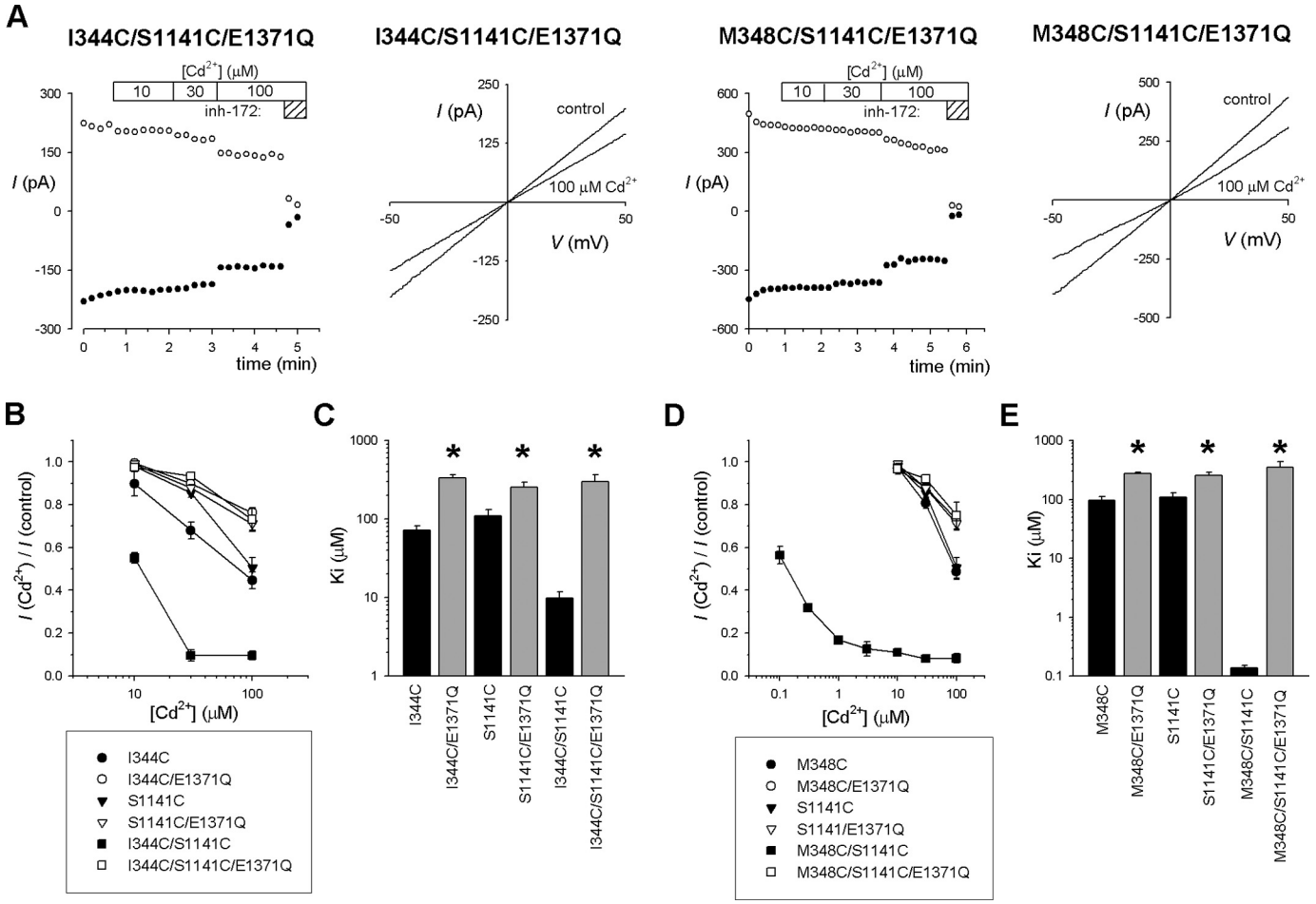

FIGURE 5. **Effect of the E1371Q mutation on the effects of Cd^{2+} on single and double cysteine mutant channels in TMs 6 and 12.** *A*, sample time courses and *I-V* curves illustrating the low Cd^{2+} sensitivity of constitutively active I344C/S1141C/E1371Q (*left panels*) and M348C/S1141C/E1371Q (*right panels*) channels in inside-out patches. Experiments were performed as described in the legend for Fig. 2. Note that although currents were relatively insensitive to Cd^{2+}, they were inhibited by $CFTR_{inh}$-172 (5 μM; indicated by *hatched bars* marked *inh-172*). *B–E*, mean fractional current remaining following the addition of different concentrations of Cd^{2+} (*B* and *D*) and mean K_i values for the single and double cysteine mutants listed (*C* and *E*). In *C* and *E*, *black bars* indicate channels gating normally, and *gray bars* indicate the corresponding cysteine mutants with the E1371Q mutation; *asterisks* indicate a significant difference between the two for the same cysteine constructs ($p < 0.02$). *Error bars* indicate the means ± S.E. from 3–7 patches.

that appears to bind Cd^{2+} ~2500 times more strongly in channels that are gating normally as compared with constitutively open E1371Q channels (Fig. 5). The unusually high apparent Cd^{2+} binding affinity of this double cysteine mutant (Figs. 3*B* and 4*B*), more than 700-fold lower K_i than the corresponding single cysteine mutants (Figs. 2*E* and 3), suggests that M348C and S1141C are uniquely well positioned to coordinate tight Cd^{2+} binding in closed channels. However, when the channel is open, these two cysteines do not appear to coordinate Cd^{2+} at all because the apparent Cd^{2+} affinity in M348C/S1141C/E1371Q channels appears the same as in M348C/E1371Q or S1141C/E1371Q (Fig. 5, *D* and *E*).

In contrast, a single identified Cd^{2+} bridge between TMs 1 and 12 (K95C/S1141C) appears to stabilize the channel open state, leading to a significant increase in channel current (Fig. 6). Because this effect was abolished in E1371Q channels (Fig. 6), it appears to reflect a Cd^{2+} bridge-induced change in channel gating rather than channel conductance. No evidence for Cd^{2+} bridge formation was observed in the limited number of TM1:TM6 double cysteine mutants that could be studied.

If we assume that the effects of Cd^{2+} bridges on the stability of the channel open and closed states reflects changes in the relative positions of cysteine side chains introduced into different TMs in these states, then our results would suggest that a number of side chains in TMs 6 and 12 are in close proximity in closed channels, and K95C (TM1) and S1141C (TM12) are in close proximity in open channels. Loss of Cd^{2+} coordination in these TM6:TM12 mutants in the open state would then reflect reduced physical proximity of these specific pairs of cysteine side chains concomitant with channel opening. What kinds of physical rearrangements of the TMs during channel gating might result in these changes in side chain relative positions?

Changes in accessibility of different side chains in TMs 6 and 12 from the cytoplasm during channel opening and closing have been interpreted as reflecting rotational movements of these TMs within the inner vestibule (11, 12). Such rotational movements could also lead to state-dependent changes in the relative positions of different side chains such as those we infer from our results. However, helical rotation alone does not appear to be able to explain the effects of Cd^{2+} bridges on chan-

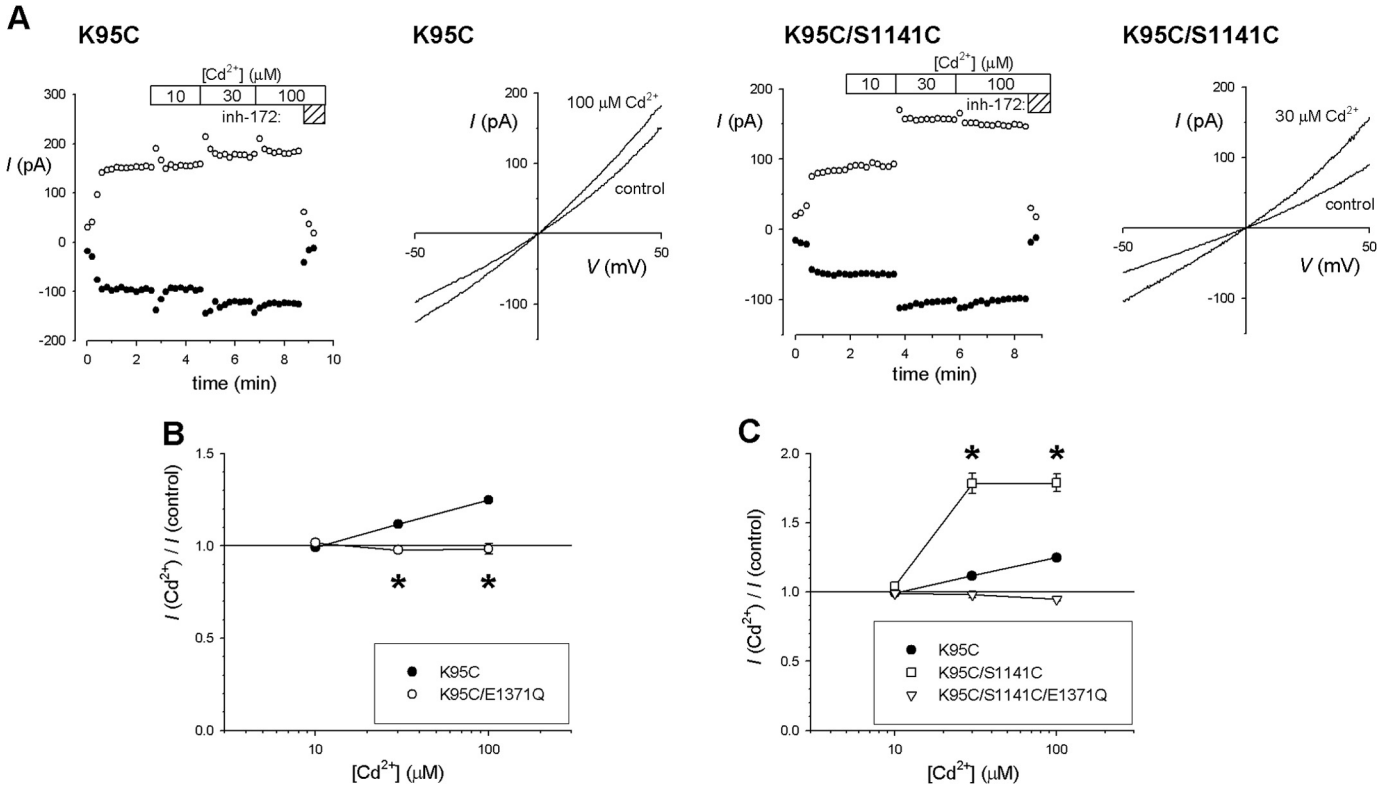

FIGURE 6. **Cadmium increases macroscopic current amplitude in K95C and K95C/S1141C channels in a gating-dependent manner.** *A*, sample time courses and *I-V* curves showing Cd^{2+} concentration-dependent increases in macroscopic current amplitude in K95C (*left panels*) and K95C/S1141C (*right panels*) channels in inside-out patches. Experiments were performed as described in the legend for Fig. 2. Note that although currents were increased by Cd^{2+}, they were inhibited by $CFTR_{inh}$-172 (5 μM). *B*, concentration-dependent increases in current amplitude in K95C were not observed in K95C/E1371Q. *Asterisks* indicate a significant difference from K95C ($p < 0.05$). *C*, Cd^{2+} causes a significantly greater increase in K95C/S1141C current amplitude as compared with K95C ($p < 0.0001$); this increase is not observed in K95C/S1141C/E1371Q channels. *Error bars* indicate the means ± S.E. from 3–6 patches.

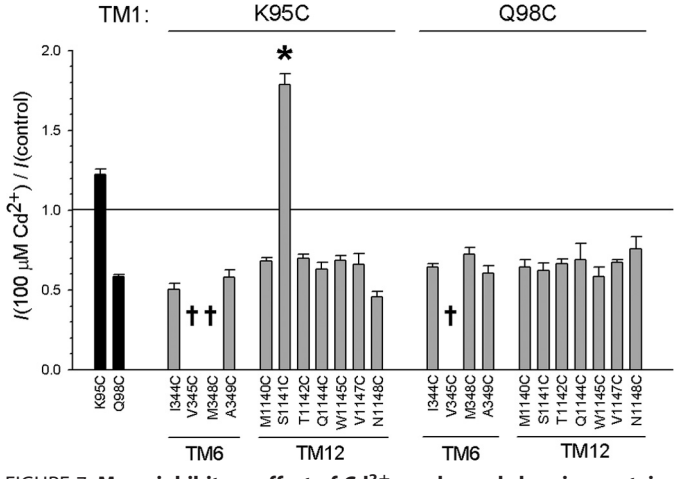

FIGURE 7. **Mean inhibitory effect of Cd^{2+} on channels bearing cysteine side chains in TM1.** Shown is the mean effect of 100 μM Cd^{2+} on macroscopic current amplitude for two single cysteine mutants (K95C, Q98C; *black bars*) and 19 double cysteine mutants that combine the TM1 cysteine listed above the panel with the TMs 6 or 12 cysteine listed below. *Daggers* indicate three mutants that did not express measureable macroscopic current in inside-out patches. *Asterisk* indicates a significant difference from the corresponding single cysteine mutant in TMs 6 or 12 ($p < 0.000005$). *Error bars* indicate the means ± S.E. from 3–5 patches.

nel gating. If the only movement of TMs 6 and 12 during channel opening and closing was a relative rotation, then we would expect some Cd^{2+} bridges to stabilize the closed state, but others (following rotation of the helices) to stabilize the open state. In fact, we found that Cd^{2+} bridges only stabilize the closed state and that these bridges appear incapable of forming in the open state. A similar argument suggests that relative translational movement of TMs 6 and 12 does not underlie channel opening and closing; if this were the case, some Cd^{2+} bridges should again be expected to stabilize the open state. Instead, we propose that the most likely physical explanation for this state-dependent Cd^{2+} bridge formation is that one face of each of TMs 6 and 12 is physically close together when the channel is closed and that these two TMs then move apart when the channel is open, such that the distance between the two TMs in the open state is too great for Cd^{2+} bridges to form between any pairs of cysteine residues exposed at this level of the pore (Fig. 8, *D* and *E*). This does not imply that these helices do not rotate and/or translate during channel opening and closing, only that the rotation and/or translation (at this level) appears coincidental to opening and closing, with physical separation and convergence of these two TMs being the mechanistically necessary conformational change that results in opening and closing. Thus, forcing TMs 6 and 12 to remain in close physical proximity (by formation of Cd^{2+} bridges between the two) stabilizes the channel closed state (Fig. 8*E*). Furthermore, this stabilization of the closed state appears relatively independent of the exact location of the Cd^{2+} bridge (Fig. 8, *A*–*C*). As described above, several different Cd^{2+} bridges can form between M348C (TM6) and TM12 (Fig. 8, *A* and *B*), as well as between S1141C (TM12) and TM6; all appear to stabilize the closed state (Figs. 3 and 4). Thus, for the reasons described earlier, there may be

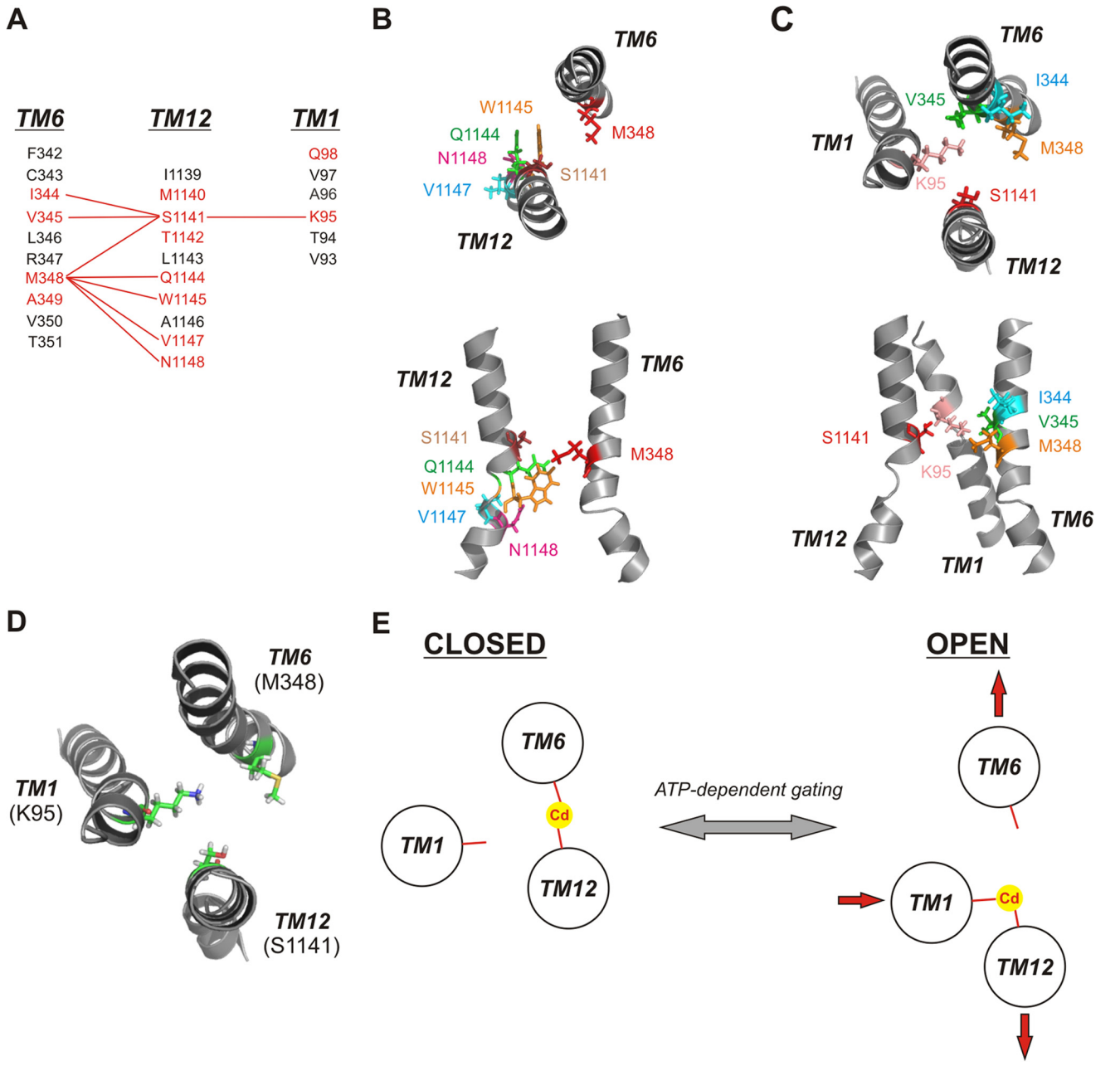

FIGURE 8. **Cadmium bridges between different TMs stabilize different channel conformations.** *A*, identification of different Cd^{2+} bridges formed between different TMs. Primary sequences of TMs 1, 6, and 12 are aligned as described previously (3). (Note: On the figure, the TMs are shown in the order (left to right) 6 - 12 - 1 for visual clarity.) Residues in *red* are those with pore-lining side chains mutated in the present study; those in *black* are non-pore-lining. *Red lines* connect residues that can form Cd^{2+} bridges following mutation to cysteine. *B*, relative location and orientation of Met-348 (TM6) with those residues in TM12, which can form Cd^{2+} bridges with M348C following mutation to cysteine. *C*, relative location and orientation of Ser-1141 (TM12) with those residues in TMs 1 and 6, which can form Cd^{2+} bridges with S1141C following mutation to cysteine. In both *B* and *C*, individual TMs are illustrated as in the atomic model of Fig. 1, viewed both from the top (*upper panels*) and from the side (*lower panels*). *D*, relative location and orientation of key Cd^{2+} bridge-forming residues Lys-95 (TM1), Met-348 (TM6), and Ser-1141 (TM12), viewed from above. *E*, proposed graphic model for Cd^{2+} bridge formation between the key sites illustrated in *D* in open and closed states, and proposed implications for conformational rearrangement of these three TMs associated with channel gating. The closed state is stabilized by a Cd^{2+} bridge between M348C (TM6) and S1141C (TM12), and the open state is stabilized by a Cd^{2+} bridge between K95C (TM1) and S1141C (TM12). In this model, ATP-dependent channel opening and closing are associated with a relative lateral movement of different TM helices (depicted by *red arrows*) with no requirement for helical rotation.

some degree of rotational and/or translational flexibility between TMs 6 and 12 in closed channels. On the other hand, maintaining the channel in the open state prevents Cd^{2+} bridge formation between cysteines in TMs 6 and 12 (Figs. 4 and 5), suggesting that these two TMs have separated during channel opening (Fig. 8*E*).

In contrast to this consistent pattern of Cd^{2+} bridge formation between TMs 6 and 12 stabilizing the closed state, a single Cd^{2+} bridge between K95C (TM1) and S1141C (TM12) appears to stabilize the open state (Fig. 6). Because only a single Cd^{2+} bridge between these TMs was identified functionally, it is difficult to draw any conclusion regarding conformational rearrangements between these TMs during channel gating. Thus, relative rotation or translational movement of these two TMs could bring these two cysteines into close proximity in the open state and separate them when the channel closes. Alter-

natively, it has been suggested that Lys-95 is not even exposed to the pore lumen when the channel is closed (14), although this suggestion is at odds with functional evidence that the native positive charge at this position can interact with cytoplasmically applied pore-blocking ions not only in the open state but also in the closed state (32). Finally, this state-dependent Cd^{2+} bridge formation could result from the same kinds of change in relative proximity of TMs 1 and 12 as we propose for TMs 6 and 12 (Fig. 8*E*). This kind of model would suggest that TMs 1 and 12 are closer together in open channels and move further apart when the channel closes (Fig. 8*E*). No evidence was obtained for Cd^{2+} bridge formation between TMs 1 and 6, and so we cannot draw any inference on proximity of these TMs in either the open or the closed state. Functional evidence suggests that Lys-95, Ile-344, Val-345, and Ser-1141 are all close together in the inner vestibule of the pore (17, 18, 32).

Our results suggest that different TMs converge and separate during channel gating, implying that ATP-dependent channel opening and closing may involve lateral movements of different TMs surrounding the inner vestibule (Fig. 8*E*). Furthermore, the physical requirement for these movements in order for channel opening and closing to proceed is underscored by the fact that constraining these movements (by the formation of Cd^{2+} bridges between different TMs) is capable of either stabilizing the closed state (preventing channel opening) or stabilizing the open state (preventing channel closing). Thus, although the conformational changes of the MSDs that underlie channel opening and closing are ultimately controlled by ATP interactions with the NBDs, these results offer encouragement that altering interactions within the MSDs themselves can, in theory, directly influence the overall activity of the CFTR channel. A substance that could influence TM:TM interactions in this way to stabilize the channel open state could theoretically represent a novel mechanism to increase CFTR function in cystic fibrosis patients.

Acknowledgment—We thank Christina Irving for technical assistance.

REFERENCES

1. Lubamba, B., Dhooghe, B., Noel, S., and Leal, T. (2012) Cystic fibrosis: insight into CFTR pathophysiology and pharmacotherapy. *Clin. Biochem.* **45,** 1132–1144
2. Hwang, T.-C., and Kirk, K. L. (2013) The CFTR ion channel: gating, regulation, and anion permeation. *Cold Spring Harb. Perspect. Med.* **3,** a009498
3. Linsdell, P. (2014) Functional architecture of the CFTR chloride channel. *Mol. Membr. Biol.* **31,** 1–16
4. Mornon, J.-P., Lehn, P., and Callebaut, I. (2008) Atomic model of human cystic fibrosis transmembrane conductance regulator: membrane-spanning domains and coupling interfaces. *Cell. Mol. Life Sci.* **65,** 2594–2612
5. Mornon, J.-P., Lehn, P., and Callebaut, I. (2009) Molecular models of the open and closed states of the whole human CFTR protein. *Cell. Mol. Life Sci.* **66,** 3469–3486
6. Dalton, J., Kalid, O., Schushan, M., Ben-Tal, N., and Villà-Freixa, J. (2012) New model of cystic fibrosis transmembrane conductance regulator proposes active channel-like conformation. *J. Chem. Inf. Model.* **52,** 1842–1853
7. Wang, W., and Linsdell, P. (2012) Relative movements of transmembrane regions at the outer mouth of the cystic fibrosis transmembrane conductance regulator channel pore during channel gating. *J. Biol. Chem.* **287,** 32136–32146
8. Wang, W., and Linsdell, P. (2012) Conformational change opening the CFTR chloride channel pore coupled to ATP-dependent channel gating. *Biochim. Biophys. Acta* **1818,** 851–860
9. Wang, W., and Linsdell, P. (2012) Alternating access to the transmembrane domain of the ATP-binding cassette protein cystic fibrosis transmembrane conductance regulator (ABCC7). *J. Biol. Chem.* **287,** 10156–10165
10. Wang, W., El Hiani, Y., Rubaiy, H. N., and Linsdell, P. (2014) Relative contribution of different transmembrane segments to the CFTR chloride channel pore. *Pflügers Arch.* **466,** 477–490
11. Bai, Y., Li, M., Hwang, T.-C. (2010) Dual roles of the sixth transmembrane segment of the CFTR chloride channel in gating and permeation. *J. Gen. Physiol.* **136,** 293–309
12. Bai, Y., Li, M., Hwang, T.-C. (2011) Structural basis for the channel function of a degraded ABC transporter, CFTR (ABCC7). *J. Gen. Physiol.* **138,** 495–507
13. Wang, W., El Hiani, Y., and Linsdell, P. (2011) Alignment of transmembrane regions in the cystic fibrosis transmembrane conductance regulator chloride channel pore. *J. Gen. Physiol.* **138,** 165–178
14. Gao, X., Bai, Y., and Hwang, T.-C. (2013) Cysteine scanning of CFTR's first transmembrane segment reveals its plausible roles in gating and permeation. *Biophys. J.* **104,** 786–797
15. El Hiani, Y., and Linsdell, P. (2010) Changes in accessibility of cytoplasmic substances to the pore associated with activation of the cystic fibrosis transmembrane conductance regulator chloride channel. *J. Biol. Chem.* **285,** 32126–32140
16. Qian, F., El Hiani, Y., and Linsdell, P. (2011) Functional arrangement of the 12th transmembrane region in the CFTR chloride channel pore based on functional investigation of a cysteine-less CFTR variant. *Pflügers Arch.* **462,** 559–571
17. Zhou, J.-J., Li, M.-S., Qi., J., and Linsdell, P. (2010) Regulation of conductance by the number of fixed positive charges in the intracellular vestibule of the CFTR chloride channel pore. *J. Gen. Physiol.* **135,** 229–245
18. El Hiani, Y., and Linsdell, P. (2012) Tuning of CFTR chloride channel function by location of positive charges within the pore. *Biophys. J.* **103,** 1719–1726
19. Webster, S. M., Del Camino, D., Dekker, J. P., and Yellen, G. (2004) Intracellular gate opening in Shaker K^+ channels defined by high-affinity metal bridges. *Nature* **428,** 864–868
20. Campos, F. V., Chanda, B., Roux, B., and Bezanilla, F. (2007) Two atomic constraints unambiguously position the S4 segment relative to S1 and S2 segments in the closed state of Shaker K channel. *Proc. Natl. Acad. Sci. U.S.A.* **104,** 7904–7909
21. Li, M., Kawate, T., Silberberg, S. D., and Swartz, K. J. (2010) Pore-opening mechanism in trimeric P2X receptor channels. *Nat. Commun.* **1,** 44
22. Henrion, U., Renhorn, J., Börjesson, S. I., Nelson, E. M., Schwaiger, C. S., Bjelkmar, P., Wallner, B., Lindahl, E., and Elinder, F. (2012) Tracking a complete voltage-sensor cycle with metal-ion bridges. *Proc. Natl. Acad. Sci. U.S.A.* **109,** 8552–8557
23. Mense, M., Vergani, P., White, D. M., Altberg, G., Nairn, A. C., and Gadsby, D. C. (2006) *In vivo* phosphorylation of CFTR promotes formation of a nucleotide-binding domain heterodimer. *EMBO J.* **25,** 4728–4739
24. Li, M.-S., Demsey, A. F. A., Qi, J., and Linsdell, P. (2009) Cysteine-independent inhibition of the CFTR chloride channel by the cysteine-reactive reagent sodium (2-sulphonatoethyl) methanethiosulphonate (MTSES). *Br. J. Pharmacol.* **157,** 1065–1071
25. Holstead, R. G., Li, M.-S., and Linsdell, P. (2011) Functional differences in pore properties between wild-type and cysteine-less forms of the CFTR chloride channel. *J. Membr. Biol.* **243,** 15–23
26. Beck, E. J., Yang, Y., Yaemsiri, S., and Raghuram, V. (2008) Conformational changes in a pore-lining helix coupled to cystic fibrosis transmembrane conductance regulator channel gating. *J. Biol. Chem.* **283,** 4957–4966
27. Gunderson, K. L., and Kopito, R. R. (1994) Effects of pyrophosphate and nucleotide analogs suggest a role for ATP hydrolysis in cystic fibrosis transmembrane conductance regulator channel gating. *J. Biol. Chem.* **269,** 19349–19353
28. Carson, M. R., Winter, M. C., Travis, S. M., and Welsh, M. J. (1995) Pyrophosphate stimulates wild-type and mutant cystic fibrosis transmembrane conductance regulator Cl^- channels. *J. Biol. Chem.* **270,**

20466–20472
29. Choi, L.-S., Mach, T., and Bayley, H. (2013) Rates and stoichiometries of metal ion probes of cysteine residues within ion channels. *Biophys. J.* **105,** 356–364
30. Ge, N., Muise, C. N., Gong, X., and Linsdell, P. (2004) Direct comparison of the functional roles played by different membrane spanning regions in the cystic fibrosis transmembrane conductance regulator chloride channel pore. *J. Biol. Chem.* **279,** 55283–55289
31. Rulísek, L., and Vondrásek, J. (1998) Coordination geometries of selected transition metal ions (Co^{2+}, Ni^{2+}, Cu^{2+}, Zn^{2+}, Cd^{2+}, and Hg^{2+}) in metalloproteins. *J. Inorg. Biochem.* **71,** 115–127
32. Linsdell, P. (2014) State-dependent blocker interactions with the CFTR chloride channel: implications for gating the pore. *Pflügers Arch.* 10.1007/s00424-014-1501-7
33. DeLano, W. L. (2010) *The PyMOL Molecular Graphics System*, version 1.3r1, Schrödinger, LLC, New York